Title
Visualizing changes in nationally averaged PM2.5 concentrations by an alluvial diagram

Journal
Environment and Planning A Economy and Space, 50(2)

ISSN
0308-518X

Authors
Liu, Ying
Zhao, Naizhuo
Vanos, Jennifer K
et al.

Publication Date
2018-03-01

DOI
10.1177/0308518x17745067

Peer reviewed

Featured graphics

A Environment and Planning

Environment and Planning A: Economy and Space
2018, Vol. 50(2) 259–261

DOI: 10.1177/0308518X17745067
journals.sagepub.com/home/epn
SAGE

Visualizing changes in nationally averaged $PM_{2.5}$ concentrations by an alluvial diagram

Ying Liu and Naizhuo Zhao
Texas Tech University, USA

Jennifer K Vanos
University of California, USA

Guofeng Cao
Texas Tech University, USA

Ailments related to ambient fine particulate matter ($PM_{2.5}$) cause 3.22 million deaths per year on average worldwide, which, along with high blood pressure and tobacco smoking, is defined as the leading risk factor for global burden of disease (Lim et al., 2013). The alluvial diagram displayed in Figure 1 demonstrates the temporal changes in the ranks of nationally averaged $PM_{2.5}$ concentrations of developed areas from 1998 to 2013 (Rosvall and Bergstrom, 2010). A 'developed area' within a country was delineated using the Defense Meteorological Satellite Program's Operational Linescan System annual stable lights image composites with pixels' digital number values equal to or larger than 10 (Zhao and Samson, 2012). A total of 46 countries with at least 10 identified developed areas in the 1998 stable lights image product are included in the alluvial diagram (Doll et al., 2000). Here each wide line in the alluvial diagram is called an alluvium. $PM_{2.5}$ concentrations were extracted from a satellite-derived gridded $PM_{2.5}$ datasets (van Donkelaar et al., 2016). This dataset is considered to be one of the most accurate global $PM_{2.5}$ concentration image products at the $0.01^\circ \times 0.01^\circ$ (or $1\,km \times 1\,km$) spatial resolution and has been used in applied public health studies (van Donkelaar et al., 2015).

Figure 1 displays differences in the width of each alluvium, which represents a country's yearly variations in $PM_{2.5}$ concentrations. The scaled width of the alluvium corresponding to the largest national average $PM_{2.5}$ concentration ($63\,\mu g/m^3$) of the 46 countries, which is found in Iraq, is marked in the diagram. In the vertical direction, the countries are ranked upward by their average $PM_{2.5}$ concentrations (from lowest to highest) for each year. The left-hand axis is ordered from the lowest to highest concentrations in 1998, while the right-hand axis is for that of 2013. Thus, a country with a drastic change in $PM_{2.5}$ concentration between the time period, such as Côte d'Ivoire, will change position substantially.

Corresponding author:
Ying Liu, Texas Tech University, Lubbock, TX 79409, USA.
Email: ying.liu@ttu.edu

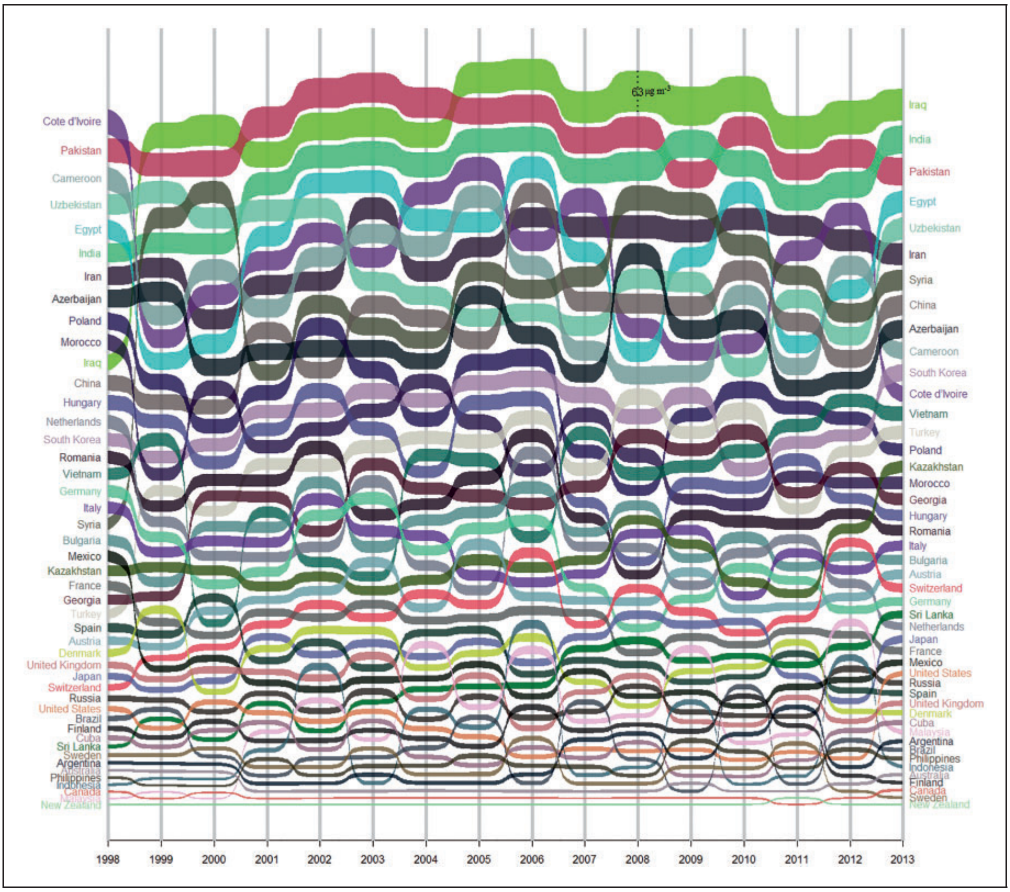

Figure 1. Rankings of nationally averaged $PM_{2.5}$ concentrations of developed areas, 1998–2013.

In the alluvial diagram, the locations with the highest $PM_{2.5}$ concentrations tend to be consistently occupied by the countries in Middle East, North Africa, and the Asian continent. The $PM_{2.5}$ concentrations of the countries with fast economic growth, such as India and China, tend to increase from 1998 to 2013. In contrast, the $PM_{2.5}$ concentrations of the European, Oceanian, American, and South Asian island countries are low in general. Furthermore, the $PM_{2.5}$ concentrations in most European countries (e.g. the United Kingdom, Germany, and Netherlands) exhibit clear decreasing trends. Interestingly, Côte d'Ivoire and Cameroon's $PM_{2.5}$ concentrations and variations across the years are relatively large, which need to be further investigated in the future. Overall, the alluvial diagram in Figure 1 is an effective method to communicate inter- and intra-country $PM_{2.5}$ concentrations within dense urban centers, allowing for identification of specific events and trends of interest by year.

Software

The nighttime lights image products and the gridded $PM_{2.5}$ datasets were processed using ArcGIS 10.4.1. The alluvial diagram was created using the package 'alluvial' in R statistical computing environment.

Declaration of conflicting interests

The author(s) declared no potential conflicts of interest with respect to the research, authorship, and/or publication of this article.

Funding

The author(s) received no financial support for the research, authorship, and/or publication of this article.

References

Doll CNH, Muller J-P and Elvidge CD (2000) Night-time imagery as a tool for global mapping of socioeconomic parameters and greenhouse gas emissions. *AMBIO* 29(3): 157–162.

Lim SS, Vos T, Flaxman AD, et al. (2013) A comparative risk assessment of burden of disease and injury attributable to 67 risk factors and risk factor clusters in 21 regions, 1990–2010: A systematic analysis for the Global Burden of Disease Study 2010. *The Lancet* 380(9859): 2224–2260.

Rosvall M and Bergstrom CT (2010) Mapping change in large networks. *PloS One* 5(1): e8694.

van Donkelaar A, Martin RV, Brauer M, et al. (2015) Global fine particulate matter concentrations from satellite for long-term exposure assessment. *Environmental Health Perspectives* 123: 135–143.

van Donkelaar A, Martin RV, Brauer M, et al. (2016) Global estimates of fine particulate matter using a combined geophysical-statistical method with information from satellites, models, and monitors. *Environmental Science & Technology* 50(7): 3762–3772.

Zhao N and Samson EL (2012) Estimation of virtual water contained in international trade products using nighttime imagery and urban population data. *International Journal of Applied Earth Observation and Geoinformation* 18: 243–250.